JACS Au
AN OPEN ACCESS JOURNAL OF THE AMERICAN CHEMICAL SOCIETY

pubs.acs.org/jacsau

Article

A DNA Aptamer That Inhibits the Aberrant Signaling of Fibroblast Growth Factor Receptor in Cancer Cells

Akihiro Eguchi, Ayaka Ueki, Junya Hoshiyama, Keiko Kuwata, Yoko Chikaoka, Takeshi Kawamura, Satoru Nagatoishi, Kouhei Tsumoto, Ryosuke Ueki,* and Shinsuke Sando*

Cite This: *JACS Au* 2021, 1, 578–585

Read Online

ACCESS | Metrics & More | Article Recommendations | Supporting Information

ABSTRACT: Growth factor receptors are activated through dimerization by the binding of their ligands and play pivotal roles in normal cell function. However, the aberrant activity of the receptors has been associated with cancer malignancy. One of the main causes of the aberrant receptor activation is the overexpression of receptors and the resultant formation of unliganded receptor dimers, which can be activated in the absence of external ligand molecules. Thus, the unliganded receptor dimer is a promising target to inhibit aberrant signaling in cancer. Here, we report an aptamer that specifically binds to fibroblast growth factor receptor 2b and inhibits the aberrant receptor activation and signaling. Our investigation suggests that this aptamer inhibits the formation of the receptor dimer occurring in the absence of external ligand molecules. This work presents a new inhibitory function of aptamers and the possibility of oligonucleotide-based therapeutics for cancer.

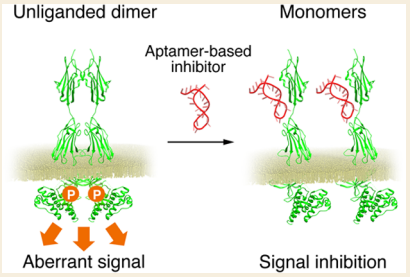

KEYWORDS: *Aptamers, Receptors, Signal Transduction, Inhibitors, Cancer*

INTRODUCTION

Growth factor receptors (GFRs) transduce cell signaling through activation and dimerization by the binding of their ligands. Receptor dimerization, a pivotal trigger in signal transduction, brings intracellular tyrosine kinase domains closer to induce their autophosphorylation. Signaling proteins are recruited to the phosphorylated sites and transduce cell signaling to the nucleus. Finally, cellular responses, such as growth and migration, are induced.[1−3] Although the dimerization and activation of the GFRs are strictly regulated by the binding of their ligands, aberrant activity of the GFRs is often observed in cancer cells. The aberrant activation of the GFRs occurs in various manners, such as autocrine or paracrine activation because of the overexpression of cognate ligands. Importantly, GFRs can also be aberrantly activated in a ligand-independent manner in GFR-overexpressing cancer cells. Because the overexpression of GFRs increases the density of receptors on the cell membrane, GFRs can form ligand-independent receptor dimers and be endogenously activated in the absence of external ligand molecules (Figure 1a).[4−6] Thus, a ligand-independent receptor dimer could be a promising target to inhibit the aberrant receptor activity in cancer cells.[4−6]

Antagonists that block the ligand−receptor interactions are good examples of inhibitors to target the ligand-dependent receptor activation. However, such competitive antagonists generally do not function as inhibitors of ligand-independent receptor activation. Therefore, dimerization inhibitors that can block the receptor−receptor interactions are necessary. For example, trastuzumab, an anti-human epidermal growth factor

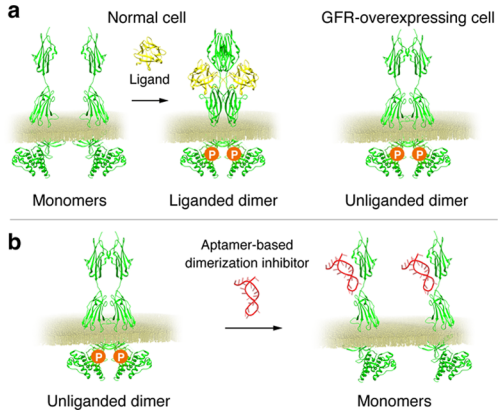

Figure 1. Schematic representation of the activation of growth factor receptor (GFR) and its inhibition. (a) GFRs are dimerized and phosphorylated by the binding of their cognate ligands. GFR-overexpression causes unliganded dimer formation and aberrant activation in cancer cells. (b) DNA aptamer that works as an inhibitor of the unliganded dimerization of GFRs. The schematic images of the receptor and ligand are depicted using data from the Protein Data Bank (PDB IDs: 3OJM and 5UR1).

Received: December 22, 2020
Published: April 8, 2021

https://doi.org/10.1021/jacsau.0c00121
JACS Au 2021, 1, 578–585

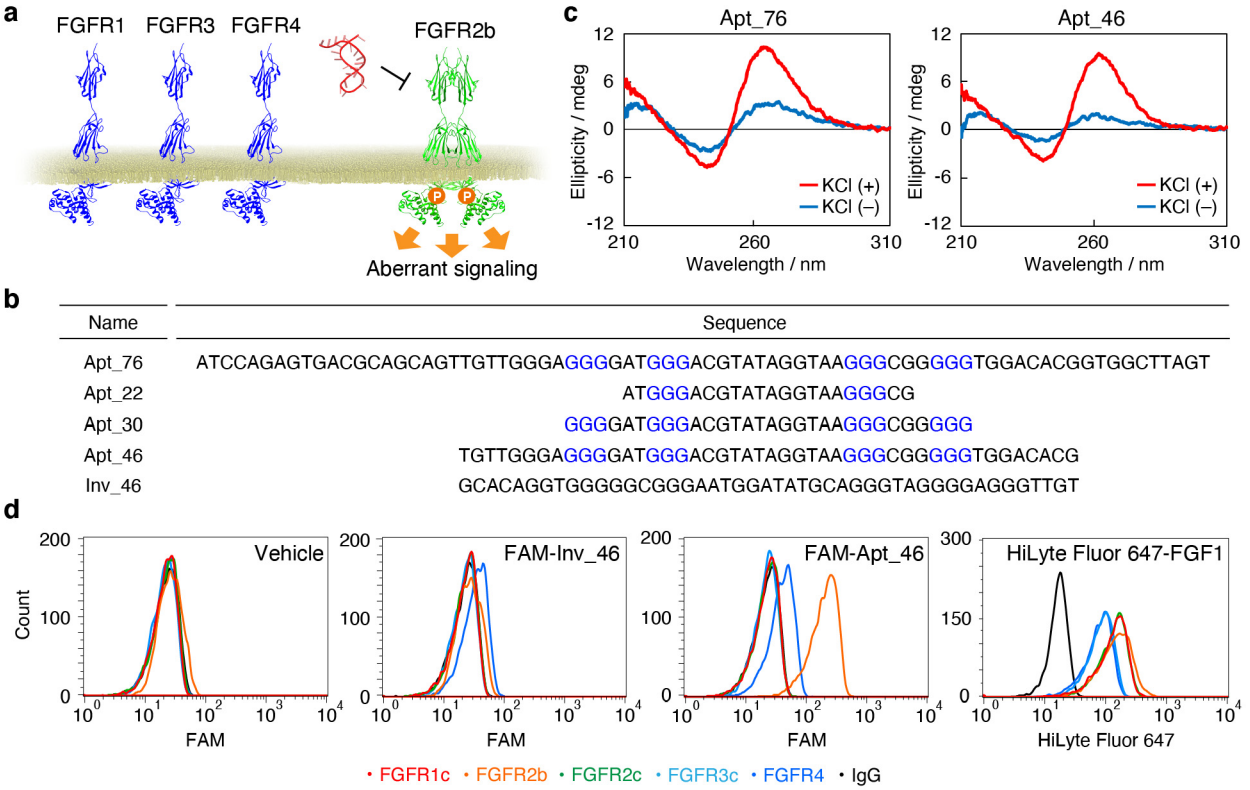

Figure 2. Selection and evaluation of an FGFR2b-binding DNA aptamer. (a) Schematic representation of aberrant signaling of overexpressed FGFR2b and its inhibition with an FGFR2b-selective DNA aptamer. (b) Full-length and truncated sequences of the FGFR2b-binding DNA aptamer candidates. G-tracts that are predicted to form a G4 structure by QGRS mapper are depicted in blue. (c) CD spectra of Apt_76 (left) and Apt_46 (right). Oligonucleotide samples (5 μM) were refolded in 20 mM Tris-HCl (pH 7.6) with (red) or without (blue) KCl (100 mM) and subjected to CD measurement at 37 °C. (d) FAM-labeled oligonucleotide samples (100 nM) or HiLyte Fluor 647-labeled FGF1 (100 nM) was incubated with FGFRs-Fc- or IgG-immobilized magnet beads for 15 min at ambient temperature. The fluorescent signal from FGFR-bound ligands was measured using flow cytometry.

receptor 2 (HER2) antibody, is known as one of the representative dimerization inhibitors.[7,8] It has been proposed that trastuzumab inhibits the formation of unliganded receptor dimers by binding to the dimer interface between HER2 and other epidermal growth factor receptor family members and prevents the endogenous activation of the receptors.[7,8] This antibody has demonstrated the therapeutic potential of dimerization inhibitors, and thus, the development of novel dimerization inhibitors based on other chemical entities would be of great interest in anticancer therapy.

Aptamers have attracted attention as a chemical alternative to antibodies. In addition to their high affinity and specificity, comparable to those of antibodies, aptamers have advantages in thermal stability, quality uniformity, and ease of preparation.[9] Various aptamers have been reported as receptor binders, including antagonists[10−15] and agonists[15−20] for GFRs. Although several reports have demonstrated that aptamers are useful for the inhibition of the ligand-dependent receptor activation, there are still significant barriers to the inhibition of the endogenous aberrant activation.

In this study, we developed a nucleic acid aptamer that can inhibit the aberrant activation of a GFR occurring in the absence of external ligand molecules. The DNA aptamer named Apt_46 inhibits the aberrant activation and downstream signaling of fibroblast growth factor receptor (FGFR) 2b in FGFR2b-overexpressing cancer cells. Furthermore, our investigation suggests that the inhibitory action is mediated by inhibition of the unliganded dimerization of FGFR2b (Figure 1b). This study suggests that a DNA aptamer-based dimerization inhibitor could be a novel class of oligonucleotide therapeutics.

RESULTS AND DISCUSSION

Target Growth Factor Receptor: FGFR2b

The FGFR family is composed of four members (FGFR1−4), and their cognate ligands, fibroblast growth factors (FGFs), comprise a 22-member family (FGF1−14 and FGF16−23).[21] Except FGFR4, FGFRs produce two splicing variants, called b-form and c-form, in which loops in Ig-like domain 3 are encoded by different exons.[21] Each FGFR member is specifically expressed in various tissues and plays an important role in the regulation of tissue- and cell-specific proliferation and development through its characteristic interaction with FGFs.[21]

FGFRs are also prominent oncogenes that are frequently overexpressed and ligand-independently activated in various cancers. As the expression profile of each FGFR type shows a distinct pattern in tissues and cell types, it is necessary to specifically inhibit only the target member of the FGFR family without affecting the activities of other FGFRs (Figure 2a). In the case of FGFR2b, gene amplification, receptor overexpression, and ligand-independent activation of FGFR2b are observed in a variety of cancer cells, such as liver, colorectal, and gastric cancers.[6,22−25] Although some tyrosine kinase inhibitor drugs against FGFRs, such as AZD4547 and

https://doi.org/10.1021/jacsau.0c00121
JACS Au 2021, 1, 578−585

BGJ398,[26−29] have been developed and are under clinical trials, these also inhibit other FGFR family members owing to the reduced specificity caused by the structural similarity of the kinase domain of FGFRs. The administration of pan-FGFRs tyrosine kinase inhibitor may cause the undesired inhibition of normal functions of FGFRs and thus has been associated with many adverse events, including hyperphosphatemia, diarrhea, ocular toxicities, and fatigue.[30] Therefore, the development of specific inhibitors for FGFR2b is of great significance.

A DNA Aptamer for FGFR2b and Its Characterization

We first selected an FGFR2b-binding DNA aptamer *in vitro* based on the systematic evolution of ligands by exponential enrichment as previously reported.[18] The selection was conducted using an N40 random DNA pool. After six rounds of selection, a highly conserved 76-mer sequence was enriched in the pool (Figure S1). We focused on the sequence as a potential FGFR2b binder and named it Apt_76 (Figure 2b). We next truncated Apt_76 into a minimal binding motif. As various DNA aptamers have been reported to adopt G-quadruplex (G4) structures,[12,31−33] we hypothesized that some guanine-tracts in the sequence would form a G4 structure and contribute to receptor binding. The analysis using QGRS Mapper[34] predicted the presence of a G4 structure within the sequence of Apt_76 (Figure 2b). The formation of the G4 structure was assessed using circular dichroism (CD) measurements in the presence or absence of potassium ions. The CD spectra of Apt_76 showed a positive peak at 265 nm and a negative peak at 240 nm (left-hand panel in Figure 2c) that were enhanced in the presence of potassium ions, which suggests the formation of a parallel G4 structure.[35] We then synthesized several truncates of Apt_76 containing or not containing the predicted G4-forming sequence (Apt_22, Apt_30, and Apt_46 in Figure 2b). Among them, only Apt_46 showed binding to FGFR2b (Figure S2) and CD spectra similar to those of Apt_76 (right-hand panel in Figure 2c). The ellipticity and binding to FGFR2b of Apt_30 and Apt_22 decreased compared with those of Apt_46 (Figures S2 and S3). From these results, we used Apt_46 as a minimal FGFR2b-binding motif for further experiments.

Next, the binding specificity of Apt_46 to FGFR2b was assessed. Protein G-conjugated magnetic beads were incubated with an Fc-chimera of FGFR1c, 2b, 2c, 3c, and 4. Human IgG was used as a negative control. These beads were subsequently incubated with FAM-labeled Apt_46, its inversed sequence (Inv_46 in Figure 2b), or HiLyte Fluor 647-labeled FGF1. FGF1 is a universal ligand against all FGFRs;[21] therefore, it was used as a positive control ligand for all FGFRs. Apt_46 showed specific binding to FGFR2b, whereas FGF1 bound to all FGFR family members (Figure 2d). Although a small amount of FGFR4 binding was observed, a similar trend was observed in Inv_46, which suggests that FGFR4 interacts with these oligonucleotides in a nonspecific manner.

We then explored the binding epitope of Apt_46 on FGFR2b. A competitive binding assay was performed using FGF10, a specific ligand for FGFR2b, the binding site for which on FGFR2b was revealed by X-ray crystallography (Figure S4).[36] The binding of FGF10 to FGFR2b decreased as the concentration of Apt_46 increased (Figure 3a), which suggests that the epitope of Apt_46 overlaps with that of FGF10. We constructed a putative dimer model of FGF10-bound FGFR2b, in which two FGF10−FGFR2b complexes (PDB ID: 1NUN) were superimposed on a known dimer

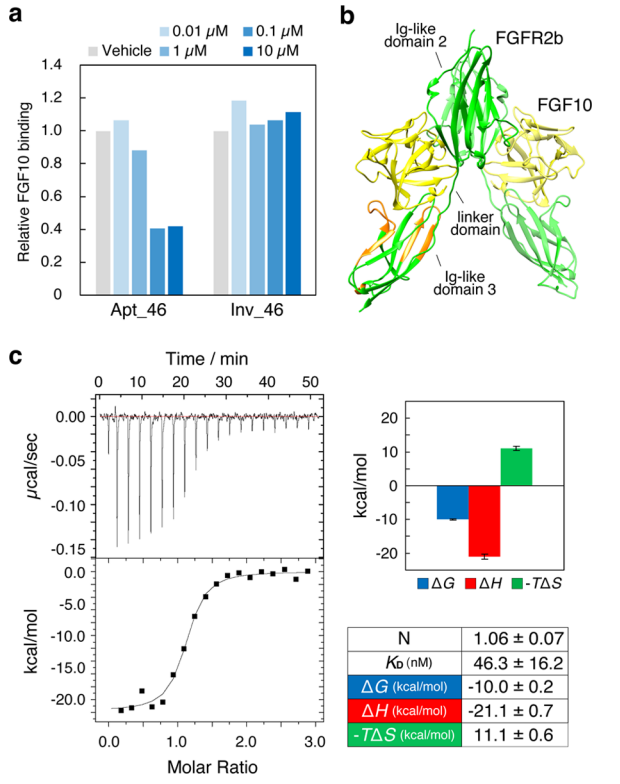

Figure 3. Characterizations of binding fashion of Apt_46 to FGFR2b. (a) Competition assay of FGF10 and Apt_46. HiLyte Fluor 647-labeled FGF10 (0.1 μM) and FAM-labeled oligonucleotide samples (0.01−10 μM) were coincubated with FGFR2b-Fc-immobilized magnet beads for 15 min at ambient temperature. The fluorescent signal of HiLyte Fluor 647-labeled FGF10 bound to the beads was measured using flow cytometry. (b) Putative model of FGFR2b dimer (green) induced by FGF10 (yellow) binding. A part of Ig-like domain 3 (orange) is encoded by different exons in FGFR2b and FGFR2c. The FGFR2b dimer complex model is built by superimposing FGFR2b−FGF10 complex structure (PDB ID: 1NUN) on a known FGFR1c−FGF2 dimer structure (PDB ID: 1FQ9). (c) Isothermal titration calorimetry measurements were conducted in Dulbecco's phosphate-buffered saline at 25 °C. The profile was obtained by the sequential titrations of Apt_46 (30 μM) to a solution of recombinant FGFR2b extracellular domain (2 μM). The parameters are shown as the mean of three measurements ± SD. A representative titration curve is shown.

structure of FGF2-bound FGFR1c (PDB ID: 1FQ9) (Figures 3b and S4). According to this structural model, FGF10 should be bound on the opposite side of the dimer interface located in Ig-like domains 2 and 3.[37] As Apt_46 did not bind to FGFR2c (Figure 2d), which is a splicing variant of FGFR2b at Ig-like domain 3 (orange-colored region in Figure 3b and sequence in Figure S5), Ig-like domain 3 is the most likely region where Apt_46 binds.

The thermodynamic parameters of Apt_46 binding to FGFR2b were measured using isothermal titration calorimetry (Figure 3c). The thermal profile was obtained by sequential titrations of Apt_46 (30 μM) to recombinant FGFR2b (2 μM) in the sample cell. We calculated stoichiometry (*N*-value), change of Gibbs free energy (Δ*G*), enthalpy (Δ*H*), and entropy (Δ*S*) based on the curve-fitting analysis of the obtained titration data. The *N*-value (1.06 ± 0.07) indicates that Apt_46 binds to FGFR2b in 1:1 stoichiometry. The dissociation constant (K_D) was 46.3 ± 16.2 nM, and the

https://doi.org/10.1021/jacsau.0c00121
JACS Au 2021, 1, 578−585

titration curve showed a large enthalpy gain (ΔH = −21.1 ± 0.7 kcal/mol) and an entropy loss ($-T\Delta S$ = 11.1 ± 0.6 kcal/mol). This result suggests that hydrogen bonds and electrostatic interactions are formed in the FGFR2b−Apt_46 interaction, which may contribute to the specific binding of the aptamer. As Apt_46 adopts a G4 structure in the presence of potassium ions (Figure 2c), we examined whether the aptamer−FGFR2b binding is correlated with the presence of potassium ions. As expected, no enthalpy-driven binding could be observed in the absence of potassium ions (Figure S6).

Intriguingly, we noticed that the N value in the ITC result increased when the measurement was conducted at higher aptamer concentrations (≥80 μM, Figure S7). We hypothesize that this phenomenon is attributed to the intermolecular dimerization of Apt_46 in high concentrations, decreasing the effective active aptamer concentration in a monomeric form. We analyzed the oligomerization state of Apt_46 using size-exclusion chromatography/multiangle light scattering (SEC-MALS) (Figure S8). The Apt_46 chromatogram showed two peaks, assigned as a monomer and a dimer based on the molecular weight. As expected, the dimer-to-monomer ratio increased as the Apt_46 concentration increased. These results suggested that Apt_46 could adopt intermolecular dimer states that do not bind to FGFR2b at high concentrations.

Inhibition of the Endogenous FGFR2b Activation and Its Putative Inhibitory Mechanism

During the characterization of Apt_46, we unexpectedly observed that Apt_46 inhibited the endogenous phosphorylation of FGFR2b in cancer cells. Previously, it was reported that FGFR2b is overexpressed and activated in gastric cancer cell lines SNU16 and KATO-III, even in the absence of external ligand molecules.[24,27,38] These cells were incubated with Apt_46, and the phosphorylation of Y656/Y657 in FGFR2b was evaluated by Western blotting (Figure 4a). Y656/Y657 are located in the activation loop of the tyrosine kinase domain, and their autophosphorylation restores the kinase activity of the receptor. Consistent with the reports,[24,27,38] FGFR2b was phosphorylated in the absence of external ligand molecules ("vehicle" lane in Figure 4a), verifying the endogenous aberrant activation occurs in these cell lines. The treatment with Apt_46 reduced the phosphorylation level of Y656/Y657 in FGFR2b in these cell lines, indicating that Apt_46 inhibited the endogenous aberrant activation and resultant kinase activity of FGFR2b overexpressed in the cancer cells. From the Western blotting analysis of phosphorylated FGFR2b at various aptamer concentrations, the apparent IC_{50} value was estimated to be approximately 200−400 nM (Figure S9).

To understand the mechanism of the inhibition, it is necessary to consider the origin of the aberrant FGFR2b activity in these cell lines. One possible cause is a ligand-dependent autocrine or paracrine activation. We measured the concentration of FGF7 and FGF10, native FGFR2b ligands, in a cell culture medium using enzyme-linked immunosorbent assay (ELISA). FGF7 and FGF10 reportedly induce DNA synthesis in Balb/MK cells from approximately 5 and 50 pM, respectively.[39] However, these ligands were not detected from the media after 24 h of KATO-III and SNU16 cell culturing (<1.7 pM for FGF7 and <0.21 pM for FGF10; data not shown). Therefore, we hypothesized that the aberrant activity of FGFR2b in these cell lines would be attributed to the formation of the unliganded receptor dimer.

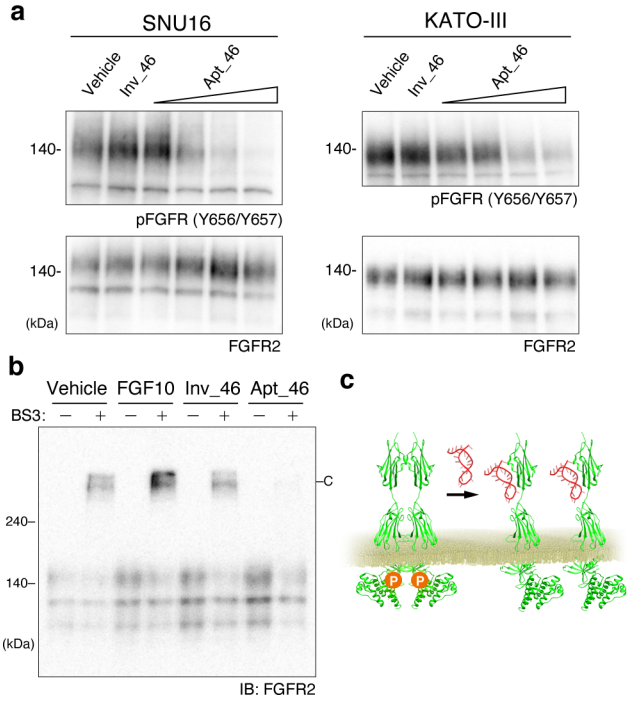

Figure 4. Inhibitory effect of Apt_46 on the aberrant FGFR2b activation. (a) Western blotting of the cell lysates of SNU16 and KATO-III cells incubated with Apt_46 (16, 80, 400, and 2000 nM) or Inv_46 (2000 nM) for 15 min. (b) Western blotting analysis of cross-linked FGFR2b dimer. SNU16 cells were incubated with FGF10 (2 nM) and heparin sodium salt (10 μg/mL), Apt_46 (1 μM), or Inv_46 (1 μM) for 1 h on ice, followed by cross-linking with BS3 (500 μM) for 1 h on ice. The cell lysates were used for Western blotting, and FGFR2b was detected. "-C" indicates the bands of cross-linked FGFR2b. (c) Apt_46 functions as an inhibitor of the unliganded FGFR2b dimer formation.

We then assessed the dimerization state of FGFR2b on the cell surface. SNU16 (Figure 4b) or KATO-III (Figure S10) cells were incubated with or without Apt_46 followed by the incubation with the chemical cross-linking agent bis-(sulfosuccinimidyl)suberate (BS3), and FGFR2b was detected by Western blotting. To inhibit receptor internalization, which might decrease receptor cross-linking efficiency with the membrane-impermeable BS3, we incubated the cells on ice for 1 h with Apt_46. In immunoblotting using an FGFR2 antibody, a new band appeared at higher molecular weight after the addition of the cross-linking agent ("-C" in Figure 4b), suggesting the formation of unliganded FGFR2b dimer. Consistently, band intensity increased upon the treatment with FGF10 that would facilitate the FGFR2b dimerization. Of note, when the cross-link was performed in the presence of Apt_46, the band at higher molecular weight was almost completely reduced, whereas the incubation with Inv_46 did not affect the cross-linking pattern. We also verified that a similar tendency was observed when the cells were incubated with Apt_46 at 37 °C (Figure S11). These results suggest that Apt_46 functions as an inhibitor of the unliganded FGFR2b dimer formation (Figure 4c).

Inhibition of the Aberrant FGFR2b Signaling in the Cancer Cells

As we confirmed that the tyrosine kinase activity of FGFR2b was inhibited by Apt_46 (Figure 4a), we investigated the inhibitory effect on FGFR2b signaling in cancer cells. We first

https://doi.org/10.1021/jacsau.0c00121
JACS Au 2021, 1, 578−585

analyzed the phosphorylation of FGFR2b intracellular domain in SNU16 cells by label-free quantitative liquid chromatography-tandem mass spectrometry (LC-MS/MS) measurements. Among the phosphorylation sites of FGFR2b detected in both Apt_46-treated and vehicle-treated samples (Figure 5a), we focused on the phosphorylated Y586/Y588 and S780,

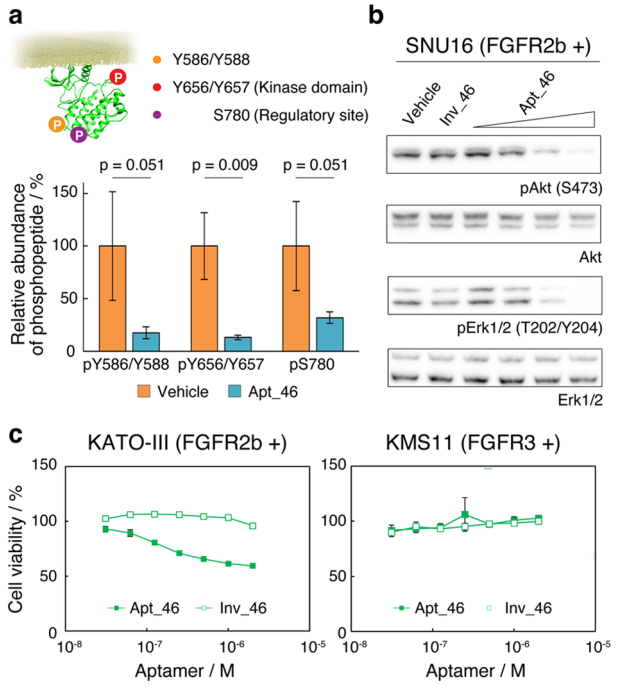

Figure 5. Inhibitory effect of Apt_46 on the aberrant activation and cell signaling in FGFR2b-overexpressing cancer cells. (a) Phosphorylation level of FGFR2b intracellular domain measured by LC-MS/MS analysis. FGFR2b was immunoprecipitated from cell lysates of SNU16 incubated with vehicle or Apt_46 (1 μM). FGFR2b protein was extracted from polyacrylamide gel after SDS-PAGE and digested by Lys-C/Trypsin, followed by LC-MS/MS analysis of phosphopeptides (refer to the Supporting Information). The bar graph shows mean ± SD (N = 3). An unpaired two-tailed t test was performed between vehicle- and Apt_46-treated conditions. The schematic illustration of intracellular FGFR2 kinase domain with detected phosphorylation sites is depicted using data from the Protein Data Bank (PDB ID: 2PSQ). (b) Western blotting of cell lysates of SNU16 cells incubated with Apt_46 (16, 80, 400, and 2000 nM) or Inv_46 (2000 nM) for 15 min. (c) Growth assay of KATO-III and KMS11 cells. Cells were cultured in the presence of 3′-inverted dT-modified Inv_46 or Apt_46 for 72 h. The initial concentration of the oligonucleotide samples was 31.3−2000 nM, and the samples were newly supplemented every 24 h (see the Supporting Information). Cell viability was measured using cell counting kit-8. The bar graph shows mean ± SD (N = 3).

as well as Y656/Y657. Y586/Y588 locate within the catalytic core of FGFR2. According to a study focused on the homologous residues in FGFR1 (Y583/Y585), these residues were suggested to be autophosphorylated after the phosphorylation of Y656.[40] S780 reportedly functions as a regulatory site for FGFR2b activity.[41] Under the experimental conditions (N = 3), the addition of Apt_46 substantially reduced the average phosphorylation levels of all the sites. We also evaluated phosphorylation of downstream signaling molecules using Western blotting. The phosphorylation levels of Akt (S473) and Erk1/2 (T202/Y204) were reduced upon the treatment with Apt_46 (Figure 5b).

To confirm the selective inhibition of FGFR2b-dependent signaling by Apt_46, we chose the FGFR3-overexpressing KMS11 cell line[26,42] for comparison (Figure S12). In flow cytometry assay, Apt_46 specifically bound to SNU16 cells and not to KMS11 cells (Figure S13). Because of its overexpression, FGFR3 is phosphorylated in the KMS11 cell line in the absence of external ligand molecules.[26,42] The phosphorylation of FGFR3 and the downstream kinases in KMS11 cells was almost unaffected by the treatment with Apt_46 (Figure S14). This is in contrast to the broad inhibitory spectrum of the pan-FGFR kinase inhibitor AZD4547, which inhibited the phosphorylation of FGFR2b or FGFR3 in each cell line (Figure S14).

Because Apt_46 inhibited cell growth-related downstream signaling proteins Akt and Erk1/2, we investigated whether Apt_46 affects the growth of SNU16 and KATO-III cells. Because we could observe Apt_46 degradation in the presence of fetal bovine serum in long-term incubation over several hours, we improved the Apt_46 serum stability by introducing a 3′-inverted dT-modification (Figure S15).[43,44] KATO-III, SNU16, and KMS11 cells were cultured in the presence of 3′-inverted dT-modified Apt_46 for 72 h, and the relative cell viability was measured (Figures 5c and S16). Under the experimental conditions, Apt_46 (IC_{50}: 171 nM) could substantially inhibit the growth of KATO-III cells (Figure 5c), whereas it did not affect KMS11 cell growth. In SNU-16 cells, cell growth could be slightly inhibited by the negative control oligonucleotide (Inv_46) at high concentrations (>1 μM; Figure S16). However, Apt_46 exerted its inhibitory effect in a low-concentration range (<1 μM), where the inhibition of FGFR2 phosphorylation was demonstrated using Western blotting (Figure S9). It was also demonstrated that the inhibitory effect of Apt_46 on FGFR2b phosphorylation lasted over several hours under the experimental conditions (Figure S17). Although the effects of the oligonucleotides on the growth of each cell line need to be considered in more detail, these results suggest that Apt_46 inhibits cancer cell growth presumably via the inhibition of the aberrant FGFR2b signaling.

Intriguingly, there was a certain gap between the IC_{50} value for cell proliferation (171 nM for KATO-III cells, Figure 5c) and the dissociation constant determined using the ITC analysis (46.3 ± 16.2 nM, Figure 3c). This implies that the affinity of Apt_46 to FGFR2b might be decreased owing to the 3′-inverted dT-modification or cell surface environments in the cell-based assay. Another possible reason might be the competition with the unliganded FGFR2b dimerization. It has been previously suggested that the FGFR2b dimerization free energy was −5.4 kcal/mol and the high FGFR2b density, because of overexpression, promotes dimerization rather than monomerization.[45] To further improve the Apt_46 inhibitory effect, affinity maturation and the chemical modification of the aptamer might be useful approaches.

CONCLUSION

In the present study, we report the DNA aptamer that inhibits the aberrant activity of FGFR2b, thereby exerting an inhibitory effect on downstream signaling. This aptamer, Apt_46, shows specific binding to FGFR2b among FGFR family members (Figure 2d) and inhibits FGFR2b-dependent signaling with high specificity compared with a pan-FGFRs tyrosine kinase inhibitor AZD4547 (Figures 4a, 5b, and S14).

https://doi.org/10.1021/jacsau.0c00121
JACS Au 2021, 1, 578−585

Specificity is an important indicator for the practical application of inhibitors. Tyrosine kinase inhibitors, which are currently major chemotherapy medications, often suffer from low specificity owing to the structural similarity of tyrosine kinase domains. AZD4547, a tyrosine kinase inhibitor of FGFRs, inhibits FGFR1−3 indistinguishably.[28] When we compared the effects of Apt_46 and AZD4547 on the intracellular phosphoproteome of SNU16, different intracellular responses were observed (Figure 6 and Table S1).

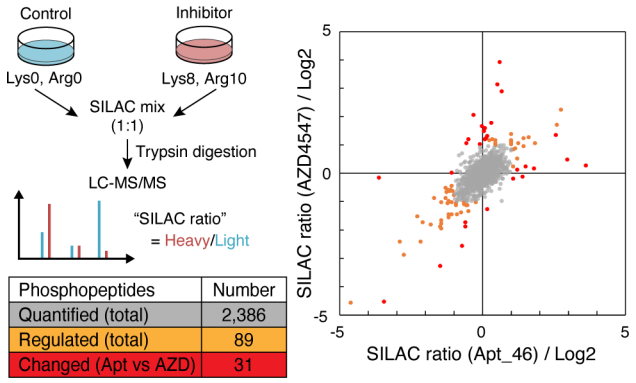

Phosphopeptides	Number
Quantified (total)	2,386
Regulated (total)	89
Changed (Apt vs AZD)	31

Figure 6. Schematic illustration of SILAC (stable isotope labeling by amino acids in cell culture)-based quantitative MS analysis. SNU16 cells grown in heavy SILAC medium were lysed using 8 M guanidium-HCl (pH 8.5) after 15 min incubation with Apt_46 (1 μM) or AZD4547 (1 μM). The cells grown in light SILAC medium were lysed after 15 min of incubation with vehicle. Three SILAC samples were prepared. Phosphopeptides that were quantified for a minimum of two of three samples in both conditions are listed. The SILAC ratio of the listed phosphopeptides is plotted in the scatter plot as "Quantified (total)" (gray). The phosphopeptides whose SILAC ratio is more than 2 or less than 0.5 in either or both of Apt_46-treated condition and AZD4547-treated condition are defined as "Regulated (total)" (orange in the scatter plot). Among "Regulated", phosphopeptides whose SILAC ratio differs more than twice between Apt_46-treated and AZD4547-treated conditions are defined as "Changed (Apt vs AZD)" (red in the scatter plot).

Under the experimental conditions, we quantified 2386 phosphopeptides ("Quantified" in Figure 6) from 1140 proteins. Among quantified phosphopeptides, there were 89 phosphopeptides whose SILAC ratio (the abundance ratio of the phosphopeptide in inhibitor-treated sample to that in vehicle-treated sample) is more than 2 or less than 0.5 in either or both of Apt_46-treated condition and AZD4547-treated condition ("Regulated" in Figure 6). Among the 89 regulated phosphopeptides, 31 phosphopeptides showed more than 2-fold different SILAC ratios between the two conditions ("Changed (Apt vs AZD)" in Figure 6). This result means that Apt_46, a specific binder to the extracellular domain of FGFR2b, shows different effect on the global phosphoproteome in cancer cells compared with AZD4547, a membrane-permeable tyrosine kinase inhibitor.

Remarkably, Apt_46 inhibited the endogenous phosphorylation of FGFR2b in cancer cells occurring in the absence of external ligand molecules. The cross-linking experiment (Figure 4b) suggests that Apt_46 functions as an inhibitor of the unliganded FGFR2b dimer formation. Although there have been many reports of aptamers that function as antagonists to inhibit ligand-dependent activation of GFRs, to the best of our knowledge, no aptamer has been demonstrated to inhibit unliganded receptor dimerization. An aptamer for the AXL receptor, a type of GFR, was reported to inhibit the endogenous activation of the AXL receptor overexpressed in a cancer cell.[13] This aptamer may inhibit the unliganded receptor dimerization, but the mechanism of action remains unclear.

It should be noted that the current experimental design cannot rule out completely the possibility that aberrant FGFR2b activation in SNU-16 and KATO-III cells occurred in a paracrine or autocrine manner. However, it is presumable that the aberrant receptor activation in the SNU16 and KATO-III cells occurs in a ligand-independent manner considering that the FGF7 and FGF10 concentrations in the culture media were lower than the biologically relevant concentrations reported in a previous study.[39] Direct methods that can assess the FGFR2b dimerization state on the cell membrane, such as an artificial membrane-based system,[45] will be useful approaches to provide direct evidence for the inhibitory mechanism of Apt_46.

While unliganded receptor dimers are important targets for cancer therapy, the structural basis of their formation remains largely unknown. This poses a challenge for the development of dimerization inhibitors and elucidation of the mechanism of their action. To establish a rational design guideline for dimerization inhibitors, future studies on the structural analysis of unliganded receptor dimers and interaction between aptamers and receptors are expected.

■ ASSOCIATED CONTENT

Supporting Information

The Supporting Information is available free of charge at https://pubs.acs.org/doi/10.1021/jacsau.0c00121.

Materials, methods, and supplementary figures and tables (PDF)

Supplementary table for the proteomics experiment (XLSX)

■ AUTHOR INFORMATION

Corresponding Authors

Ryosuke Ueki − *Department of Chemistry and Biotechnology, The University of Tokyo, Tokyo 113-8656, Japan;* orcid.org/0000-0002-5433-5354; Email: r.ueki@chembio.t.u-tokyo.ac.jp

Shinsuke Sando − *Department of Chemistry and Biotechnology and Department of Bioengineering, The University of Tokyo, Tokyo 113-8656, Japan;* orcid.org/0000-0003-0275-7237; Email: ssando@chembio.t.u-tokyo.ac.jp

Authors

Akihiro Eguchi − *Department of Chemistry and Biotechnology, The University of Tokyo, Tokyo 113-8656, Japan*

Ayaka Ueki − *Department of Chemistry and Biotechnology, The University of Tokyo, Tokyo 113-8656, Japan*

Junya Hoshiyama − *Department of Chemistry and Biotechnology, The University of Tokyo, Tokyo 113-8656, Japan*

Keiko Kuwata − *Institute of Transformative Bio-Molecules (WPI-ITbM), Nagoya University, Nagoya, Aichi 464-8601, Japan*

Yoko Chikaoka − *Proteomics Laboratory, Isotope Science Center, The University of Tokyo, Tokyo 113-0032, Japan*

https://doi.org/10.1021/jacsau.0c00121
JACS Au 2021, 1, 578−585

Takeshi Kawamura − *Proteomics Laboratory, Isotope Science Center, The University of Tokyo, Tokyo 113-0032, Japan*
Satoru Nagatoishi − *The Institute of Medical Science, The University of Tokyo, Tokyo 108-8639, Japan;* orcid.org/0000-0002-0794-3963
Kouhei Tsumoto − *Department of Chemistry and Biotechnology, The Institute of Medical Science, and Department of Bioengineering, The University of Tokyo, Tokyo 113-8656, Japan;* orcid.org/0000-0001-7643-5164

Complete contact information is available at: https://pubs.acs.org/10.1021/jacsau.0c00121

Notes

The authors declare no competing financial interest.
Raw data of LC-MS/MS measurements (RAW) is available upon request.

■ ACKNOWLEDGMENTS

The expression vector pEFs[46] was kindly provided by Prof. Yamashita (Yokohama City University). The authors thank Dr. Tamura (Kyoto University) for helpful advice about the data analysis of quantitative proteomics. The authors also thank Dr. Goto and Prof. Suga (The University of Tokyo) for the use of CD spectrometry. This work was supported by grants from the Asahi Glass Foundation for S.S.; a Grant-in-Aid for Young Scientists (#19K15693) from the Japan Society for the Promotion of Science (JSPS), Adaptable and Seamless Technology transfer Program through Target-driven R&D (#JPMJTR20UL, A-STEP) from Japan Science and Technology Agency (JST), and a Noguchi-Shitagau Research Grant from The Noguchi Institute for R.U.; and partly supported by AMED under Grant Number JP20ak0101139 for S.S. and JP20am0101094 for K.T.; ITbM is supported by the World Premier International Research Center Initiative, Japan.

■ REFERENCES

(1) Yarden, Y.; Ullrich, A. Growth factor receptor tyrosine kinases. *Annu. Rev. Biochem.* **1988**, *57*, 443−478.
(2) Claesson-Welsh, L. Platelet-derived growth factor receptor signals. *J. Biol. Chem.* **1994**, *269*, 32023−32026.
(3) Bogdan, S.; Klämbt, C. Epidermal growth factor receptor signaling. *Curr. Biol.* **2001**, *11*, R292−R295.
(4) Worthylake, R.; Opresko, L. K.; Wiley, H. S. ErbB-2 amplification inhibits down-regulation and induces constitutive activation of both ErbB-2 and epidermal growth factor receptors. *J. Biol. Chem.* **1999**, *274*, 8865−8874.
(5) Shinomiya, N.; Gao, C. F.; Xie, Q.; Gustafson, M.; Waters, D. J.; Zhang, Y. W.; Vande Woude, G. F. RNA interference reveals that ligand-independent met activity is required for tumor cell signaling and survival. *Cancer Res.* **2004**, *64*, 7962−7970.
(6) Turner, N.; Pearson, A.; Sharpe, R.; Lambros, M.; Geyer, F.; Lopez-Garcia, M. A.; Natrajan, R.; Marchio, C.; Iorns, E.; Mackay, A.; Gillett, C.; Grigoriadis, A.; Tutt, A.; Reis-Filho, J. S.; Ashworth, A. FGFR1 amplification drives endocrine therapy resistance and is a therapeutic target in breast cancer. *Cancer Res.* **2010**, *70*, 2085−2094.
(7) Franklin, M. C.; Carey, K. D.; Vajdos, F. F.; Leahy, D. J.; de Vos, A. M.; Sliwkowski, M. X. Insights into ErbB signaling from the structure of the ErbB2-pertuzumab complex. *Cancer Cell* **2004**, *5*, 317−328.
(8) Junttila, T. T.; Akita, R. W.; Parsons, K.; Fields, C.; Lewis Phillips, G. D.; Friedman, L. S.; Sampath, D.; Sliwkowski, M. X. Ligand-independent HER2/HER3/PI3K complex is disrupted by trastuzumab and is effectively inhibited by the PI3K inhibitor GDC-0941. *Cancer Cell* **2009**, *15*, 429−440.
(9) Zhou, J.; Rossi, J. Aptamers as targeted therapeutics: current potential and challenges. *Nat. Rev. Drug Discovery* **2017**, *16*, 181−202.
(10) Chen, C. H. B.; Chernis, G. A.; Hoang, V. Q.; Landgraf, R. Inhibition of heregulin signaling by an aptamer that preferentially binds to the oligomeric form of human epidermal growth factor receptor-3. *Proc. Natl. Acad. Sci. U. S. A.* **2003**, *100*, 9226−9231.
(11) Li, N.; Nguyen, H. H.; Byrom, M.; Ellington, A. D. Inhibition of cell proliferation by an anti-EGFR aptamer. *PLoS One* **2011**, *6*, e20299.
(12) Ueki, R.; Sando, S. A DNA aptamer to c-Met inhibits cancer cell migration. *Chem. Commun.* **2014**, *50*, 13131−13134.
(13) Kanlikilicer, P.; Ozpolat, B.; Aslan, B.; Bayraktar, R.; Gurbuz, N.; Rodriguez-Aguayo, C.; Bayraktar, E.; Denizli, M.; Gonzalez-Villasana, V.; Ivan, C.; Lokesh, G. L. R.; Amero, P.; Catuogno, S.; Haemmerle, M.; Wu, S. Y. Y.; Mitra, R.; Gorenstein, D. G.; Volk, D. E.; de Franciscis, V.; Sood, A. K.; Lopez-Berestein, G. Therapeutic Targeting of AXL Receptor Tyrosine Kinase Inhibits Tumor Growth and Intraperitoneal Metastasis in Ovarian Cancer Models. *Mol. Ther.–Nucleic Acids* **2017**, *9*, 251−262.
(14) Wang, L.; Liang, H.; Sun, J.; Liu, Y.; Li, J.; Li, J.; Li, J.; Yang, H. Bispecific Aptamer Induced Artificial Protein-Pairing: A Strategy for Selective Inhibition of Receptor Function. *J. Am. Chem. Soc.* **2019**, *141*, 12673−12681.
(15) Kamatkar, N.; Levy, M.; Hébert, J. M. Development of a Monomeric Inhibitory RNA Aptamer Specific for FGFR3 that Acts as an Activator When Dimerized. *Mol. Ther.–Nucleic Acids* **2019**, *17*, 530−539.
(16) Ramaswamy, V.; Monsalve, A.; Sautina, L.; Segal, M. S.; Dobson, J.; Allen, J. B. DNA Aptamer Assembly as a Vascular Endothelial Growth Factor Receptor Agonist. *Nucleic Acid Ther.* **2015**, *25*, 227−234.
(17) Ueki, R.; Ueki, A.; Kanda, N.; Sando, S. Oligonucleotide-Based Mimetics of Hepatocyte Growth Factor. *Angew. Chem., Int. Ed.* **2016**, *55*, 579−582.
(18) Ueki, R.; Atsuta, S.; Ueki, A.; Hoshiyama, J.; Li, J.; Hayashi, Y.; Sando, S. DNA aptamer assemblies as fibroblast growth factor mimics and their application in stem cell culture. *Chem. Commun.* **2019**, *55*, 2672−2675.
(19) Yoshitomi, T.; Hayashi, M.; Oguro, T.; Kimura, K.; Wayama, F.; Furusho, H.; Yoshimoto, K. Binding and Structural Properties of DNA Aptamers with VEGF-A-Mimic Activity. *Mol. Ther.–Nucleic Acids* **2020**, *19*, 1145−1152.
(20) Ueki, R.; Uchida, S.; Kanda, N.; Yamada, N.; Ueki, A.; Akiyama, M.; Toh, K.; Cabral, H.; Sando, S. A chemically unmodified agonistic DNA with growth factor functionality for in vivo therapeutic application. *Sci. Adv.* **2020**, *6*, eaay2801.
(21) Ornitz, D. M.; Itoh, N. The Fibroblast Growth Factor signaling pathway. *WIREs Dev. Biol.* **2015**, *4*, 215−266.
(22) Katoh, Y.; Katoh, M. FGFR2-related pathogenesis and FGFR2-targeted therapeutics. *Int. J. Mol. Med.* **2009**, *23*, 307−311.
(23) Matsuda, Y.; Ueda, J.; Ishiwata, T. Fibroblast growth factor receptor 2: expression, roles, and potential as a novel molecular target for colorectal cancer. *Patholog. Res. Int.* **2012**, *2012*, 574768.
(24) Jo, J. C.; Choi, E. K.; Shin, J. S.; Moon, J. H.; Hong, S. W.; Lee, H. R.; Kim, S. M.; Jung, S. A.; Lee, D. H.; Jung, S. H.; Lee, S. H.; Kim, J. E.; Kim, K. P.; Hong, Y. S.; Suh, Y. A.; Jang, S. J.; Choi, E. K.; Lee, J. S.; Jin, D. H.; Kim, T. W. Targeting FGFR Pathway in Human Hepatocellular Carcinoma: Expressing pFGFR and pMET for Antitumor Activity. *Mol. Cancer Ther.* **2015**, *14*, 2613−2622.
(25) Ahn, S.; Lee, J.; Hong, M.; Kim, S. T.; Park, S. H.; Choi, M. G.; Lee, J. H.; Sohn, T. S.; Bae, J. M.; Kim, S.; Jung, S. H.; Kang, W. K.; Kim, K. M. FGFR2 in gastric cancer: protein overexpression predicts gene amplification and high H-index predicts poor survival. *Mod. Pathol.* **2016**, *29*, 1095−1103.
(26) Gavine, P. R.; Mooney, L.; Kilgour, E.; Thomas, A. P.; Al-Kadhimi, K.; Beck, S.; Rooney, C.; Coleman, T.; Baker, D.; Mellor, M. J.; Brooks, A. N.; Klinowska, T. AZD4547: An Orally Bioavailable,

Potent, and Selective Inhibitor of the Fibroblast Growth Factor Receptor Tyrosine Kinase Family. *Cancer Res.* **2012**, *72*, 2045−2056.
(27) Chang, J.; Wang, S.; Zhang, Z.; Liu, X.; Wu, Z.; Geng, R.; Ge, X.; Dai, C.; Liu, R.; Zhang, Q.; Li, W.; Li, J. Multiple receptor tyrosine kinase activation attenuates therapeutic efficacy of the fibroblast growth factor receptor 2 inhibitor AZD4547 in FGFR2 amplified gastric cancer. *Oncotarget* **2015**, *6*, 2009−2022.
(28) Chae, Y. K.; Ranganath, K.; Hammerman, P. S.; Vaklavas, C.; Mohindra, N.; Kalyan, A.; Matsangou, M.; Costa, R.; Carneiro, B.; Villaflor, V. M.; Cristofanilli, M.; Giles, F. J. Inhibition of the fibroblast growth factor receptor (FGFR) pathway: the current landscape and barriers to clinical application. *Oncotarget* **2017**, *8*, 16052−16074.
(29) Perez-Garcia, J.; Muñoz-Couselo, E.; Soberino, J.; Racca, F.; Cortes, J. Targeting FGFR pathway in breast cancer. *Breast* **2018**, *37*, 126−133.
(30) Mahipal, A.; Tella, S. H.; Kommalapati, A.; Yu, J.; Kim, R. Prevention and treatment of FGFR inhibitor-associated toxicities. *Crit. Rev. Oncol. Hematol.* **2020**, *155*, 103091.
(31) Macaya, R. F.; Schultze, P.; Smith, F. W.; Roe, J. A.; Feigon, J. Thrombin-binding DNA aptamer forms a unimolecular quadruplex structure in solution. *Proc. Natl. Acad. Sci. U. S. A.* **1993**, *90*, 3745−3749.
(32) Nonaka, Y.; Sode, K.; Ikebukuro, K. Screening and Improvement of an Anti-VEGF DNA Aptamer. *Molecules* **2010**, *15*, 215−225.
(33) Fujita, H.; Imaizumi, Y.; Kasahara, Y.; Kitadume, S.; Ozaki, H.; Kuwahara, M.; Sugimoto, N. Structural and Affinity Analyses of G-Quadruplex DNA Aptamers for Camptothecin Derivatives. *Pharmaceuticals* **2013**, *6*, 1082−1093.
(34) Kikin, O.; D'Antonio, L.; Bagga, P. S. QGRS Mapper: a web-based server for predicting G-quadruplexes in nucleotide sequences. *Nucleic Acids Res.* **2006**, *34*, W676−W682.
(35) Gray, D. M.; Wen, J. D.; Gray, C. W.; Repges, R.; Repges, C.; Raabe, G.; Fleischhauer, J. Measured and calculated CD spectra of G-quartets stacked with the same or opposite polarities. *Chirality* **2008**, *20*, 431−440.
(36) Yeh, B. K.; Igarashi, M.; Eliseenkova, A. V.; Plotnikov, A. N.; Sher, I.; Ron, D.; Aaronson, S. A.; Mohammadi, M. Structural basis by which alternative splicing confers specificity in fibroblast growth factor receptors. *Proc. Natl. Acad. Sci. U. S. A.* **2003**, *100*, 2266−2271.
(37) Zinkle, A.; Mohammadi, M. Structural Biology of the FGF7 Subfamily. *Front. Genet.* **2019**, *10*, 102.
(38) Kunii, K.; Davis, L.; Gorenstein, J.; Hatch, H.; Yashiro, M.; Di Bacco, A.; Elbi, C.; Lutterbach, B. FGFR2-amplified gastric cancer cell lines require FGFR2 and Erbb3 signaling for growth and survival. *Cancer Res.* **2008**, *68*, 2340−2348.
(39) Igarashi, M.; Finch, P. W.; Aaronson, S. A. Characterization of recombinant human fibroblast growth factor (FGF)-10 reveals functional similarities with keratinocyte growth factor (FGF-7). *J. Biol. Chem.* **1998**, *273*, 13230−13235.
(40) Furdui, C. M.; Lew, E. D.; Schlessinger, J.; Anderson, K. S. Autophosphorylation of FGFR1 kinase is mediated by a sequential and precisely ordered reaction. *Mol. Cell* **2006**, *21*, 711−717.
(41) Szybowska, P.; Kostas, M.; Wesche, J.; Wiedlocha, A.; Haugsten, E. M. Cancer Mutations in FGFR2 Prevent a Negative Feedback Loop Mediated by the ERK1/2 Pathway. *Cells* **2019**, *8*, 518.
(42) Chell, V.; Balmanno, K.; Little, A. S.; Wilson, M.; Andrews, S.; Blockley, L.; Hampson, M.; Gavine, P. R.; Cook, S. J. Tumour cell responses to new fibroblast growth factor receptor tyrosine kinase inhibitors and identification of a gatekeeper mutation in FGFR3 as a mechanism of acquired resistance. *Oncogene* **2013**, *32*, 3059−3070.
(43) Dass, C. R.; Saravolac, E. G.; Li, Y.; Sun, L. Q. Cellular uptake, distribution, and stability of 10−23 deoxyribozymes. *Antisense Nucleic Acid Drug Dev.* **2002**, *12*, 289−299.
(44) Maier, K. E.; Levy, M. From selection hits to clinical leads: progress in aptamer discovery. *Mol. Ther.–Methods Clin. Dev.* **2016**, *3*, 16014.
(45) Sarabipour, S.; Hristova, K. Mechanism of FGF receptor dimerization and activation. *Nat. Commun.* **2016**, *7*, 10262.
(46) López-Perrote, A.; Castaño, R.; Melero, R.; Zamarro, T.; Kurosawa, H.; Ohnishi, T.; Uchiyama, A.; Aoyagi, K.; Buchwald, G.; Kataoka, N.; Yamashita, A.; Llorca, O. Human nonsense-mediated mRNA decay factor UPF2 interacts directly with eRF3 and the SURF complex. *Nucleic Acids Res.* **2016**, *44*, 1909−1923.

https://doi.org/10.1021/jacsau.0c00121
JACS Au 2021, 1, 578−585